

# Comparing GPS-Constrained Forward and Inverse Models of Volume Change at The Geysers, CA

Rachel Terry<sup>1</sup>, Gareth J. Funning<sup>1</sup>, and Michael A. Floyd<sup>2</sup>

<sup>1</sup>University of California, Riverside, <sup>2</sup>Massachusetts Institute of Technology

## Keywords

*GPS, The Geysers, Reservoir Modeling, Geothermal, Injection, Subsidence, Surface Deformation, Elastic Dislocation Modeling*

## ABSTRACT

The Geysers geothermal field in northern California has seen subsidence, attributed to net volume loss during power production, since at least the 1960s. Over the last three decades this has been accompanied by reductions in reservoir steam pressure and power generation. To combat these effects, wastewater has been injected in the field since 1997. In order to better understand the effects of variations in production and wastewater injection on geothermal reservoir volume and surface subsidence over time, we installed two continuously-recording GPS stations (TG01 and TG02) in the northern Geysers in 2012 and one in the southern Geysers (TG03) in 2013.

We present here our first analyses of the continuous GPS data. Combining these data with data from seven PBO GPS stations in the region, we first use common-mode filtering to remove any regionally-correlated seasonal noise from our GPS time series. Both TG01 and TG02 show early periods of uplift and later subsidence while TG03 shows ongoing subsidence. Next, we downsample steam extraction and injection data onto a rectangular grid and calculate ‘observed’ monthly volume changes as a function of position. We then use these to drive a forward elastic dislocation model to predict surface deformation changes each month in The Geysers field. This forward model overpredicts subsidence at all three Geysers GPS locations.

We then compare the observed volume changes with inverse elastic dislocation models of the volume changes required to reproduce the GPS time series. We find that our GPS data do not have sufficient spatial resolution to reproduce the variability in reservoir volume change from reported well data. However, the estimates of total volume change from the inverse models and

well data are comparable in amplitude and show periods where the peaks in each are in phase, and periods where they are out of phase. In these cases, the peaks in the inverse modeled volume changes lag those in the reported data by one month. These 'out-of-phase periods' correlate with periods of peak injection in the field, typically in the winter and early spring months, suggesting that the GPS data are detecting a delayed deformation response to injection in the field, possibly related to the finite permeability of the geothermal reservoir rocks.

## 1. Introduction

The Geysers geothermal field (The Geysers) in northern California has been in commercial operation since 1960 and is currently the largest producing geothermal field in the world. In its early history, power production at The Geysers steadily increased, reaching a peak of ~2 GW in 1987 and then a more notable decrease in power production/shut down of power plants in the late 1980s and early 1990s. The reduction in power output is a result of declining steam pressures (3.4MPa to 1.2MPa) within the reservoir and is assumed to be due to production volumes and rates exceeding restoration of reservoir volumes by natural means (e.g. Gettings et al., 2002; Calpine, 2018). Evaporative steam loss is common in geothermal fields and can impact the long-term sustainability of the field.

Surface subsidence has been monitored at The Geysers over the past few decades by geodetic means. In the 1970s, leveling surveys indicated surface subsidence of up to 13 cm in 4.5 years in the area of highest steam withdrawals (e.g. Lofgren, 1978). In the 1990s, Mossop and Segall (1997) revisited previous leveling monuments with GPS receivers and measured subsidence rates of up to 4.8 cm/yr. Most recently, campaign GPS surveys recorded a reduction in subsidence rate following the introduction of wastewater pipelines into The Geysers field, with the most significant velocity changes occurred within 1-2 km of large injection sites (e.g. Floyd & Funning 2013).

The two wastewater injection pipelines, completed in 1997 and 2003, deliver an average of 15 million gallons per day to The Geysers area and were installed to combat the declining steam pressures. Since introduction of these pipelines, energy production has stabilized and as of 2017, the average output was 648 MW (Calpine, 2018). Due to the episodic nature of GPS campaign measurements (typically separated in time by multiple years), much was not known about the time dependence of subsidence/uplift due to production activities on shorter, daily-to-monthly time scales. Therefore, in December 2012, we installed two continuous GPS stations in The Geysers field, and added another in December 2013. With the capability to continuously measure surface deformation changes, we can learn more about the connection between reservoir changes and surface deformation and how or whether GPS could be used as a tool to monitor geothermal fields in the future.

In this paper, we present our first analyses of the continuous GPS data and our first attempts at using simple elastic dislocation models to reproduce the GPS time series data. We compute forward models using steam extraction and water injection monthly totals to predict surface displacements and inverse models using the monthly changes in vertical and horizontal positions from the GPS data to infer reservoir volume changes. We compare the model displacements with

our GPS time-series displacements each month to see the fit of the model. We then compare the forward and inverse models' total volume changes each month in The Geysers.

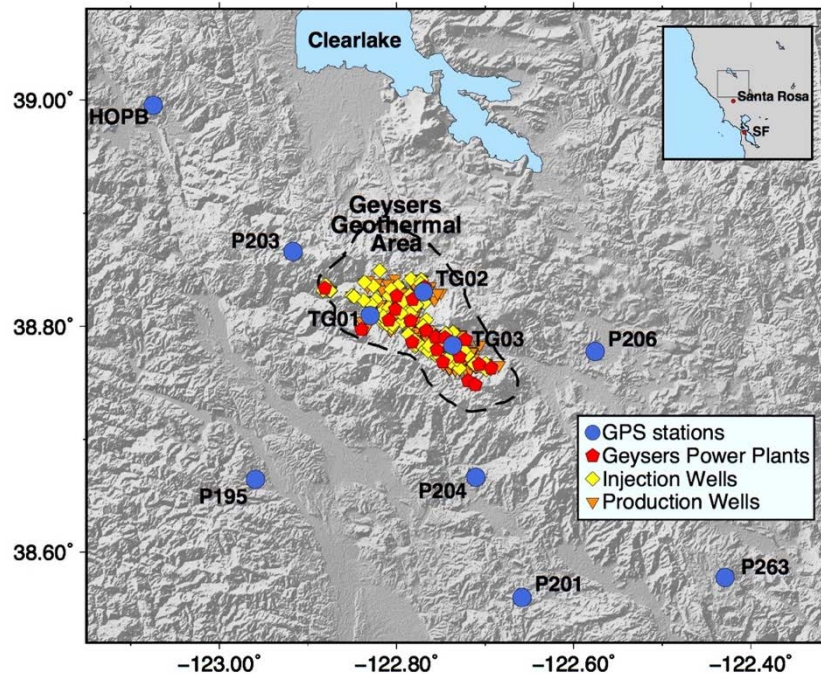


**Figure 1: Overview of The Geysers geothermal field and surrounding area. The blue circles indicate the PBO and The Geysers (within geothermal area – black dashed line) three continuous GPS stations, TG01, TG02, and TG03. Injection wells (yellow diamonds), production wells (orange triangles) and power plants (red pentagons) are also shown. Inset shows location of map area in context to surrounding area (black box).**

## 2. Methods

### 2.1 GPS Data

#### 2.1.1 GPS Data Processing

We installed two continuous GPS stations (TG01 and TG02) in the northern section of The Geysers geothermal field in December 2012 and one more station (TG03) in the southern section in December 2013. These sites are telemetered and push data daily to the Northern California Earthquake Data Center at UC Berkeley, from where it is downloaded to MIT and processed. The daily data are processed using the GAMIT/GLOBK software suite (Herring et al., 2015),

with IGS final orbits and atmospheric loading applied to improve accuracy and reduce scatter of the vertical component (e.g. Tregoning and Watson, 2009, 2011). Nearby sites from the Plate Boundary Observatory (e.g. “P” sites in Figure 1) and other sites further afield in the western hemisphere are included in the processed network to stabilize the resulting time series in the terrestrial reference frame. The sites surrounding The Geysers are also used to define a local reference frame, where the velocities of the surrounding sites are minimized to reveal the motions within The Geysers relative to the immediate surroundings.

### 2.1.2 GPS Time Series

Daily time series relative to this local reference frame are shown in Figure 2 for our three sites in The Geysers and P203, just to the northwest. It is immediately evident that all sites in the northern part (P203, TG01, TG02) show uplift of a few cm/year until around fall 2014 (bottom plot, whereafter all sites subside at a rate of several mm/yr (bottom plot of Figure 2). This also coincides with a distinct change in horizontal motion, seen particularly clearly in the “flattening” of the north component of TG01 (green time series in Figure 2), where it used to move southwards at a rate of about 1 cm/yr.

In this study, we focus on the period from 2013-2016. During this time, the GPS station TG01, located in the northwest portion of the field record uplift of ~40 mm from December 2012 to September 2014, subsidence of ~25mm from September 2014 to October 2016, and resumed uplift from October 2016 until February 2017. It also recorded continuous southward and eastward movement of ~40 mm over the 4-year period. The GPS Station TG02, located in the northeast portion of the field recorded shorter periods of uplift and subsidence of ~10-20 mm between December 2012 and September 2014 and then subsided ~40 mm from September 2014 to November 2016, and had a short period of uplift of ~5-10 mm from November 2016 to February 2017. It also recorded an almost continuous southward movement of ~50 mm but only ~5 mm of eastward movement. The GPS station TG03, the only station located in the southern portion of the field, was the last GPS station to be installed in December 2013 and was offline for the time period between September 2015 and December 2016. Despite the gap in time, TG03 showed continuous subsidence of ~60 mm and short periods of northward and southward movement of ~10 mm, but an overall southward movement of ~15 mm and eastward movement of ~20 mm.

### 2.1.3 Correcting for Seasonal Motions

A common signal in GPS time series data is seasonal motion due to hydrological loading and other variations. Such signals are expected to be fairly consistent over an area larger than The Geysers. Therefore, we remove a common seasonal signal estimated using common-mode filtering (Wdowinski et al., 1997) of data from six regional plate boundary observatory (PBO) GPS stations within 100 km of The Geysers geothermal area. The PBO station P203 was not included as part of the regional signal as its time series shows abnormal movement during the time interval of the northwest Geysers Enhanced Geothermal Systems demonstration project (Garcia et al., 2012), which is the type of local deformation signal we are attempting to retain while correcting for regional fluctuations. The seasonal correction estimated using the other six PBO stations is shown in Figure 3.

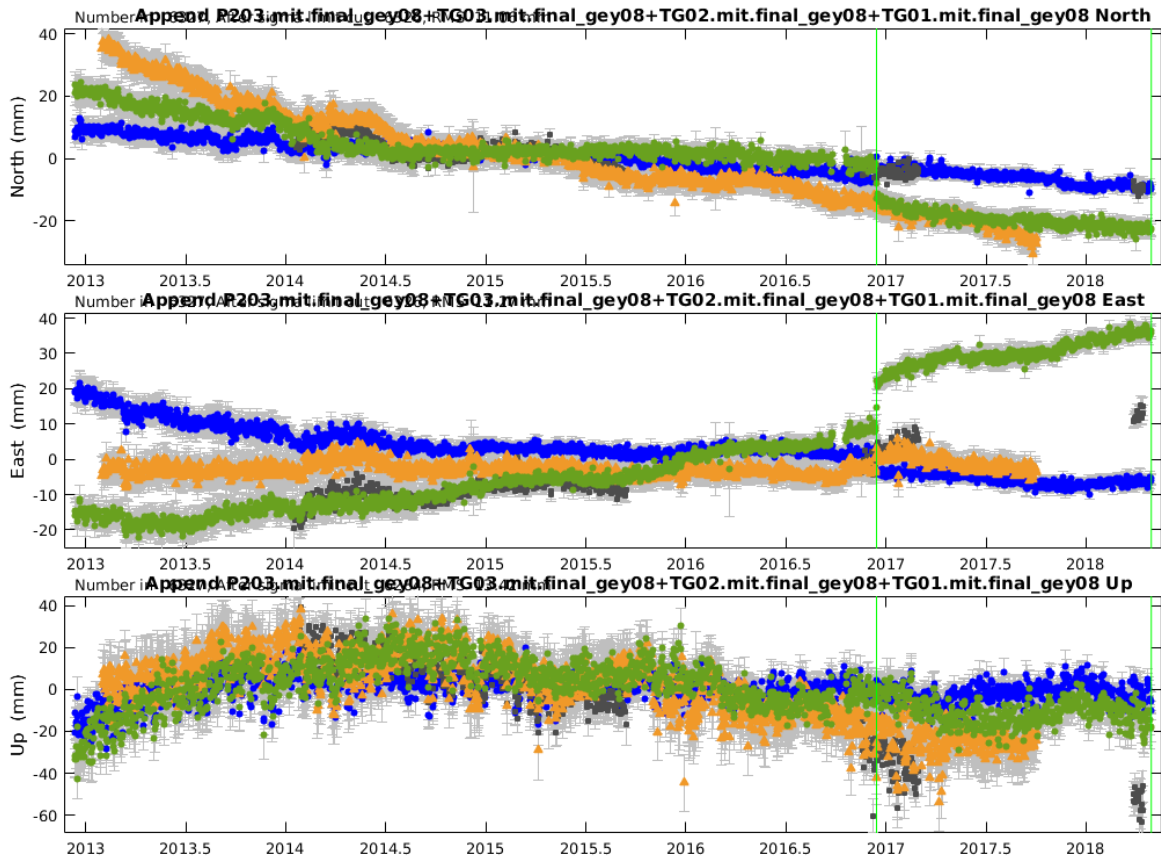


Figure 2: Time series for four sites (P203, blue; TG01, green; TG02, orange; and TG03, gray) expressed a local reference frame. Typical seasonal (annual) fluctuation are seen superimposed on the general trends and changes in trend. The green vertical line, at which an offset is seen in at least the green TG01 and blue P203 time series, corresponds to the December 14, 2016  $M_w$  5.0 earthquake.

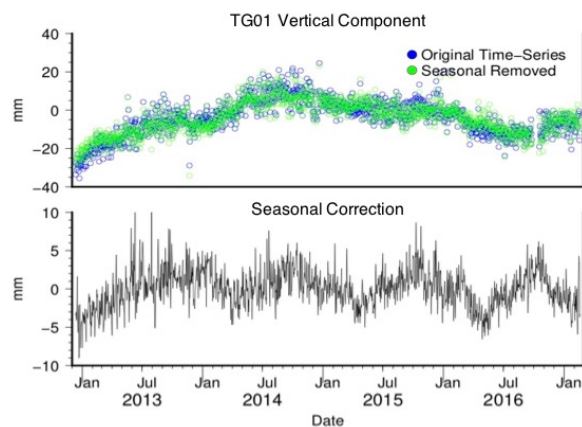
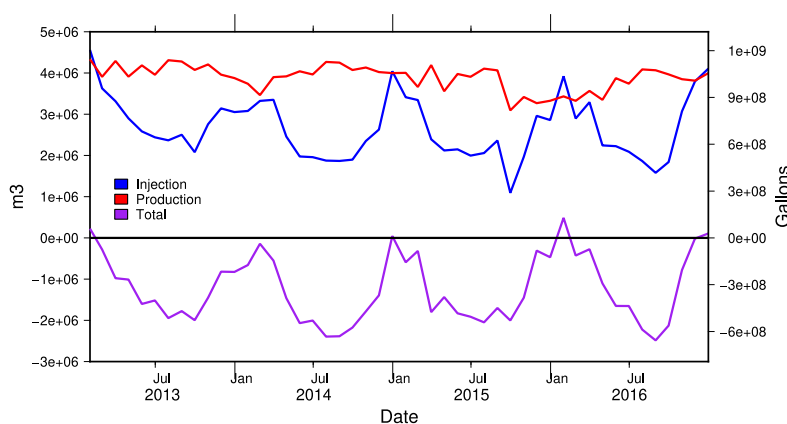


Figure 3: The vertical component time series of the GPS station TG01 with (green, top) and without (blue, top) common-mode filtering of seasonal signals. The seasonal correction (black, bottom), estimated using the six PBO stations within 100 km of The Geysers, shows an average hydrological loading amplitude of  $\sim 10$  mm. This correction once removed from the vertical components of The Geysers GPS time series reduces the variation in position.

## 2.2 Steam Extraction and Wastewater Injection Well Data

Steam extraction (production) and water/wastewater injection well data for years 2013 – 2016 were obtained from the California Department of Conservation, Division of Oil, Gas and Geothermal Resources e.g. CA Dept. Of Conservation (2017). The total number of drilled production and injection wells in The Geysers area is 396 and 96, respectively, but not all wells were in use during the 2013 – 2016 period. Since well records are reported on a monthly basis, our model data input is limited to monthly gross injected volumes and gross steam volumes. The total monthly production, injection and total (production minus injection) are shown in Figure 4. Water injection in The Geysers is seasonally modulated, with the greatest injection volumes in the winter season when precipitation is the highest. Production remains approximately constant over the four-year period and is larger in amplitude than injection for almost all months.



**Figure 4: Total monthly production (red), injection (blue) and combined (production minus injection, purple) for all active geothermal wells within The Geysers geothermal field from 2013 to 2016. Injection is seasonally modulated with highest volumes in the winter months, while production remains approximately constant over the four year period. Production volumes are consistently higher than injection for almost all months during this time period.**

To deal with the large number of wells in close proximity to one another and simplify the modeling process, we apply two downsampling approaches (Figure 5). First, we created a 1.5 x 1.5 km grid across The Geysers field, and second, we grouped the wells into three main areas (northwest section, north section and south section). For the remainder of this paper, we will refer to the 1.5 x 1.5 km grid as the 'fine grid' and the three-area grid as the 'coarse grid'. We sum monthly gross steam extraction and injection volumes for each grid cell and use these totals as inputs in our forward model calculations, described below.

## 2.3 Forward and Inverse Models

To assess the relationships between our time series of surface displacements, as measured by our GPS stations, and volume changes within the geothermal reservoir, we compute two types of model. We use our downsampled monthly injection and production volume data to calculate *forward models* of the surface deformation that might be expected as a result. Then, we use our GPS deformation time series to estimate *inverse models* of the reservoir volume changes that best explain those data. In both model types, we compute Green's functions relating reservoir

opening to surface displacement, assuming opening on rectangular elastic dislocations within an isotropic elastic half space (Okada, 1985), one within each cell of our downsampling grids, testing the coarse and fine grids separately. We test two alternative configurations of these dislocations within each cell – a horizontal opening sill, and a pair of conjugate vertical dikes. A visual representation of these dislocations is shown in Figure 6.

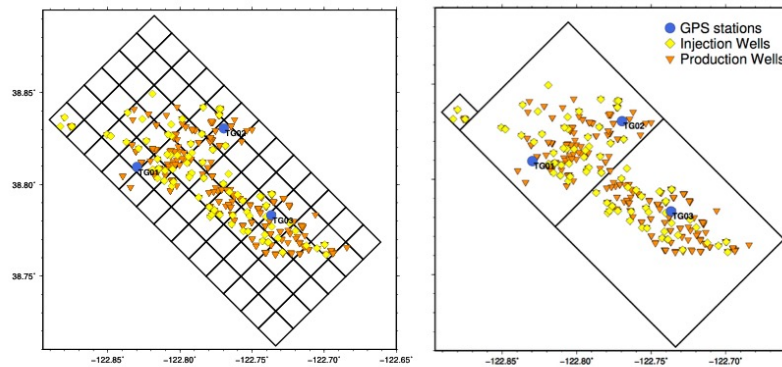


**Figure 5: Two gridding schemes used to downsample well data, with a 1.5 x 1.5 km grid on the left (fine grid) and a 3 section grid (coarse grid) on the right, indicated by black outlines. Each grid cell with wells was summed for their total injection and extraction volumes. Injection (yellow diamonds), production (orange triangles) and the three continuous GPS stations (blue circles) are also shown.**

For the coarse grid, the location for each dislocation in each cell is centered on the effective 'center of mass' of volume change for that cell for the 48 month period, computed using the extraction and injection volumes and their corresponding well locations. The surface length of each dislocation is the distance from the northernmost well to the southernmost well in each section and is 1 km for the NW cell, 6.4 km for the N cell and 8 km for the SE cell. For the fine grid, each dislocation is 1.45 km and each center is the geographic center of each grid cell. The width of each dislocation is 3 km and is based on the average width of the reservoir and the center of dislocation is located at a depth of 3.5 km. The strike used for horizontal dislocation models is  $335^\circ$  and is based on the NW-SE trending direction of The Geysers geothermal field and the strikes used for the two vertical dislocations is  $335^\circ$  and  $65^\circ$ . We assume a Poisson's ratio of 0.25 for all models.

For each forward model, we input (separately) total injection and extraction volumes for each month, and, using the areas of the dislocations being modeled, estimate the amount of dislocation-normal displacement (opening or closing) required to match those volumes. We then use these to compute monthly vertical and horizontal surface displacements at each GPS station location due to each dislocation in them model and sum them to get the total displacement each month. This monthly deformation is cumulatively summed and compared to our GPS time series for the same time period and the root-mean-square (RMS) misfit is calculated to evaluate the fit.

For the inverse model, using the monthly deformation time series from our three GPS stations and the seven surrounding PBO stations, we invert using our elastic Green's functions for the

dislocation-normal displacement required to reproduce the GPS time series displacements each month. For the fine grid model, which, given the large number of model parameters, would otherwise be an underdetermined model, we use a truncated singular value decomposition to reduce the rank deficiency of the model; although a stable inverse model is obtained through this procedure, this stability comes at the expense of reduced spatial resolution in the model. The coarse model is inverted using a standard least-squares method. We run two inverse models for each grid/dislocation model, one that includes TG03 time series data when it is available and one using only TG01 and TG02 data. To keep from having a significant number of time series to compare, we use the opening values from the inverse model with TG03 when available in conjunction with the opening values without TG03. We then compare the total volume change each month between the forward and inverse model, and also compare the modeled GPS deformation time series against the data.

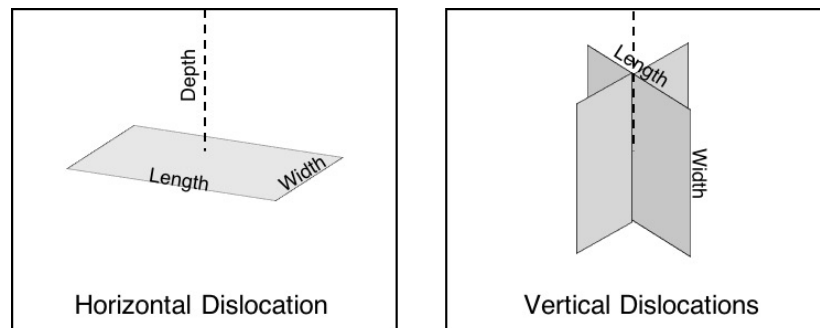


**Figure 6: Visual representation of the horizontal and vertical dislocations used in our models, showing the definitions of length, width and depth in each case.**

### 3. Results & Discussion

#### 3.1 Forward Model

The GPS time series compared with the four model time series are shown in Figure 7. No model accurately and consistently reproduces all three components of the GPS time series, but the conjugate vertical dislocation models fit significantly better, with an average RMS misfit 6 times lower than the horizontal dislocation models. Both models that use horizontal dislocations produce very large subsidences – up to 200 mm at the GPS TG01 station, 400 mm at TG02 and 700 mm at TG03. The horizontal dislocations do produce a more noticeable seasonal trend that is reflected in the vertical GPS components at TG01 and TG02 but the uplift produced in the model occurs 3-4 months prior to any uplift in the corresponding GPS time series. The models based upon conjugate vertical dislocations produced similar displacements over the 2013-2016 period and more closely reflect the change in vertical position of all GPS stations, but do not reproduce the overall uplift at TG01. When comparing the fine and coarse grid dislocation models, the fine grid has a lower RMS misfit at all GPS stations locations.

The conjugate vertical dislocation models also provide a better fit with the GPS data than the horizontal dislocation model which have 2 times higher average RMS misfit values. The gridding method used does not have a significant effect on the fit of the vertical dislocation model time series. Alongside their large vertical component misfits, the horizontal dislocation models also greatly overestimate horizontal movement in both the north and east component and at all GPS stations except for the north component TG03 and the east component of TG02.

Overall, the horizontal dislocation models accounted for the highest RMS misfit values for all components except TG01 east and TG03 north, for which the vertical dislocation model RMS misfit values were not significantly higher. Due to the large differences between the RMS misfit values between the vertical and horizontal dislocation models, we prefer the vertical dislocation models. Evaluating the dislocation gridding methods, the overall better fit for the vertical displacements is from the fine grid, as the RMS misfit averaged over all components is 12.1 mm vs 12.9 mm for the coarse grid. Although the vertical dislocation models are better at reproducing the GPS time series data, there is still room for improvement. Currently, the possibility of fluid migration within the reservoir, which may cause surface deformation farther away from the source, is not considered as dislocations are only present where wells currently exist. Also, poroelastic changes and changes in compressibility within the reservoir over time may change the magnitude of deformation over time.

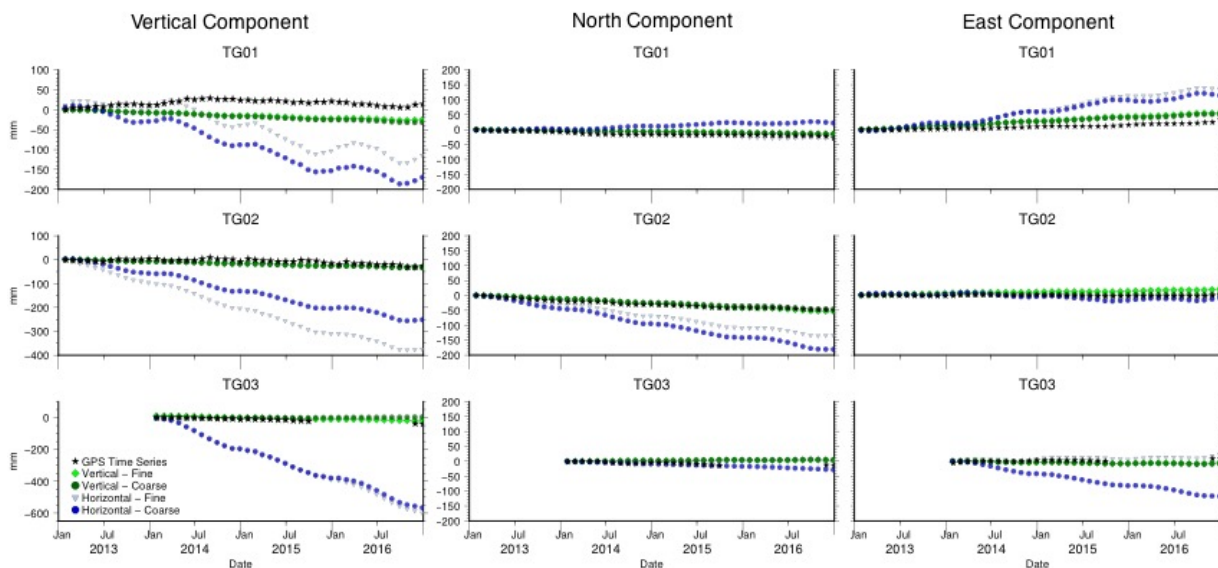


**Figure 7: Cumulatively summed monthly model displacements each of the four forward models compared with the GPS time series vertical, north and east components. No model can accurately predict both the horizontal and vertical components of the GPS time series but the conjugate vertical dislocations (greens) on both the coarse and fine grid are better at predicting all components of the GPS time series.**

### 3.2 Inverse Model

Our inverted model time series are shown in Figure 8. The inverted horizontal dislocation fine grid model reproduces the vertical component very well at all three locations, with the lowest RMS misfit (4-5 mm) of all models. The vertical dislocation inverse models produce displacements that are smaller in magnitude than those from vertical GPS time series, but that follow the general trend. The vertical dislocation models also put little (<20 mm) displacement on the north and east components. Overall, the inverse models have significantly lower average RMS misfit values for both horizontal dislocation inverse models than for the forward models, but are not significantly better or worse for the vertical dislocation models.

To compare the spatial distribution of dislocation-normal displacement across the field between the forward and inverse models, we plotted their distributions in Figure 9. The downsampled well data has large amplitude, short wavelength variations in the spatial distribution of volume changes, both negative and positive in sign. The inverse model cannot resolve this level of variation and instead places smaller dislocation-normal displacements over wider areas, suggesting that a denser deployment of GPS stations and/or a dense set of displacement measurements from a complementary technique such as InSAR would be necessary to capture some of the finer details of volume change in the field. Given the lack of resolution across the model, we find that the overall total volume change each month provides a more robust metric for comparison of the models; we compare these below.

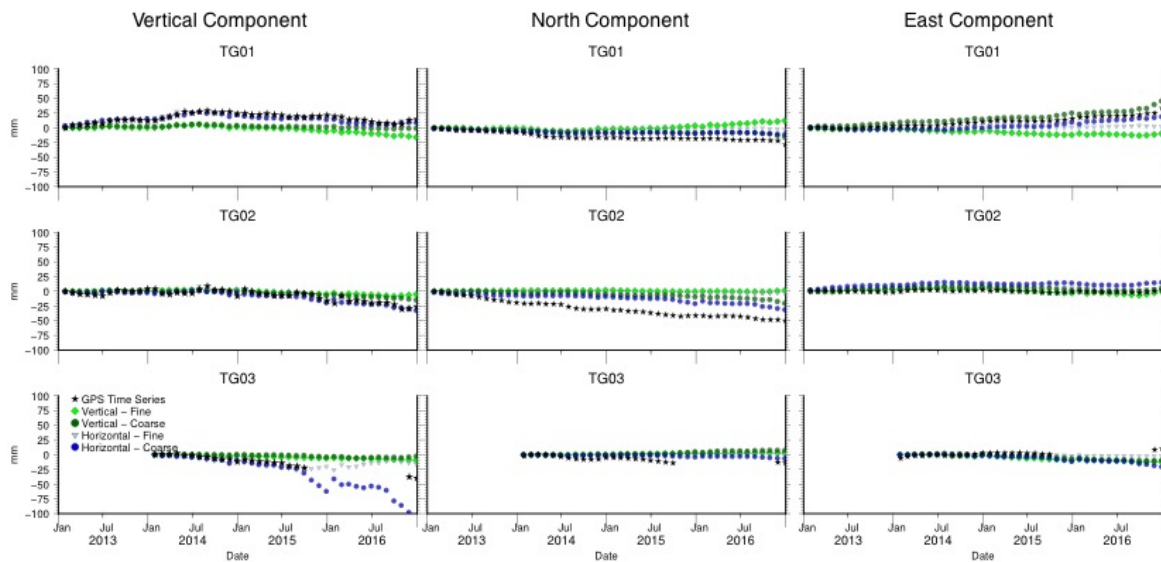


**Figure 8: Cumulatively summed monthly model displacements for each of the four inverse models compared with the GPS time series vertical, north and east components. RMS misfit values are significantly reduced for the horizontal dislocation inverse models compared with the forward models. There is not a significant reduction in RMS misfit values for the vertical dislocation models.**

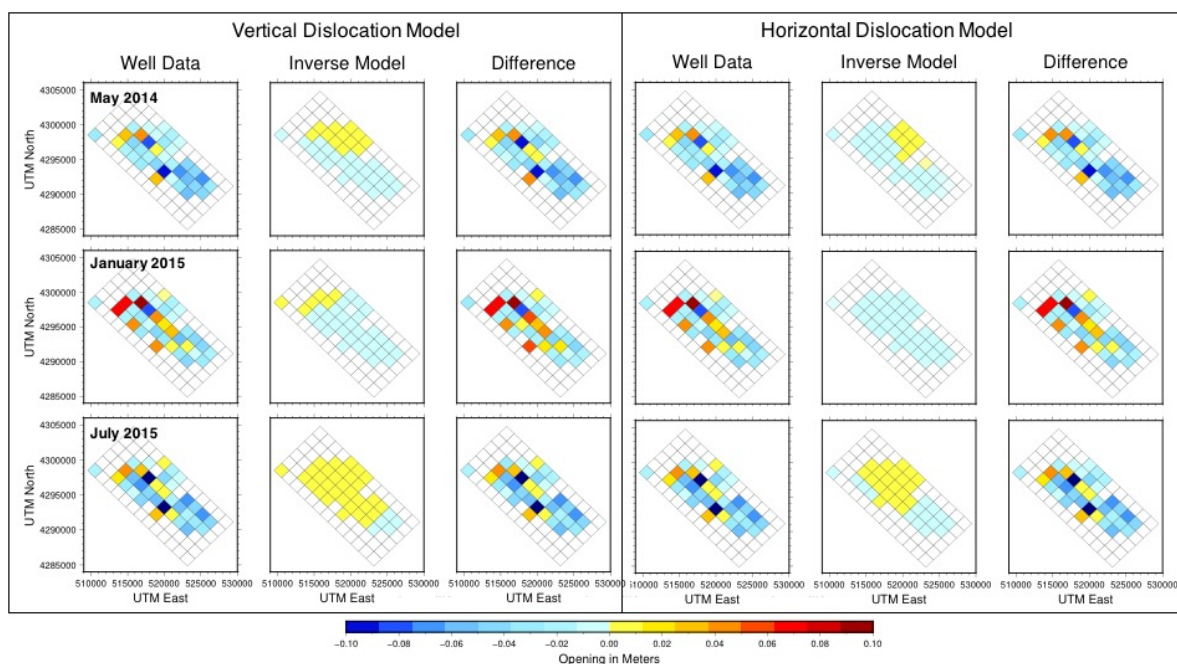


**Figure 9: Comparison of the forward openings obtained by well data and the inverted openings (dislocation-normal displacements) for May 2014, January 2015 and July 2015. All months shown are during the period when TG03 was recording its position. Here we show both the fine grid model with conjugate vertical dislocations (left) and the corresponding model with horizontal dislocations (right). The low spatial resolution of the inverse models results in smaller values of opening across a wider area than the highly variable values obtained from the well data.**

### 3.3 Total Volume Change

The total volume change between each month from all inverse models and from The Geysers field are shown in Figure 10. All models produce similar volume changes throughout all 48 months. The only model that varies significantly is the fine grid with horizontal dislocations when TG03 data are excluded, as it has very small volume changes each month. Once TG03 is introduced in the model, it produces similar volume changes.

For all inverse models, there are periods of several months where the estimated volume changes are in phase with the reported volume change within The Geysers field (Figure 10A), and periods where they are out of phase by one month (with the reported values showing a peak one month before the inverse modeled values). These out-of-phase periods are marked by large amplitude differences between the reported and modeled volume time series, particularly notable between January and April in 2015 and 2016 in all inverse models (Figure 10); in phase periods, in contrast, show smaller differences, for example between May and October 2015 (Figure 10). These out of phase periods are temporally correlated with periods of high injection across the field (Figure 11). This coincidence in time with peak injection and the one-month phase lag of the models with respect to the total volume change may indicate a delayed surface deformation response to large changes in volume injected into the reservoir, possibly related to the finite permeability of the rocks of the geothermal reservoir.

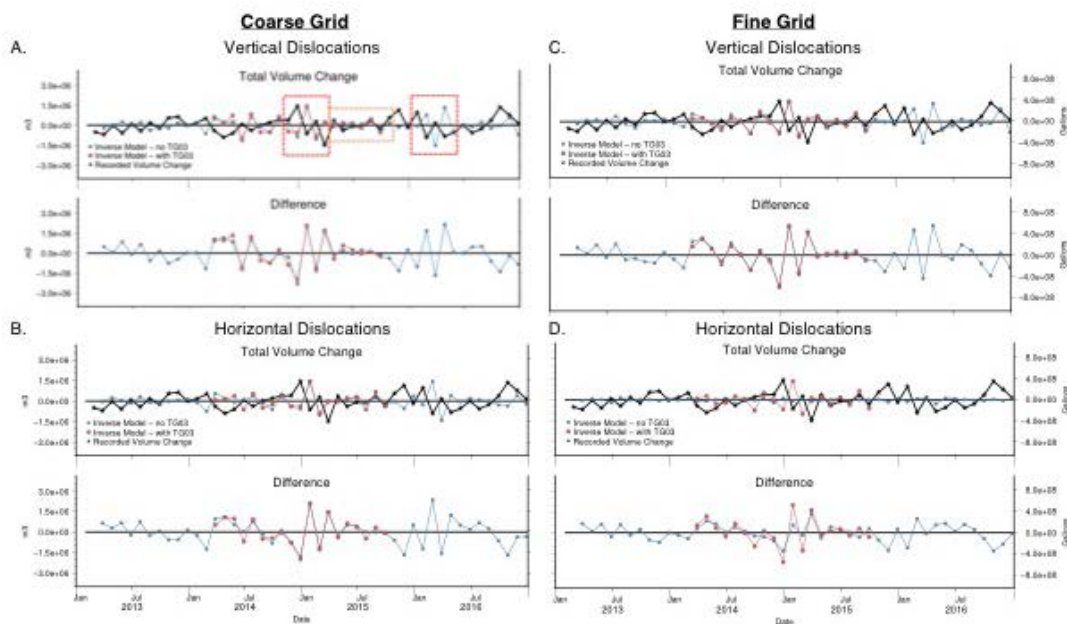


Figure 10: Comparison of the total volume change recorded from steam extraction and water injection in The Geysers field each month from 2013 to 2016 (black) and the total volume change in the inverse model using the GPS displacement data (with TG03 – red / without TG03 – blue) for all four models. Notable times when a phase shift occurs (red boxes) and when the model is in phase (orange box) in all models are shown in A.

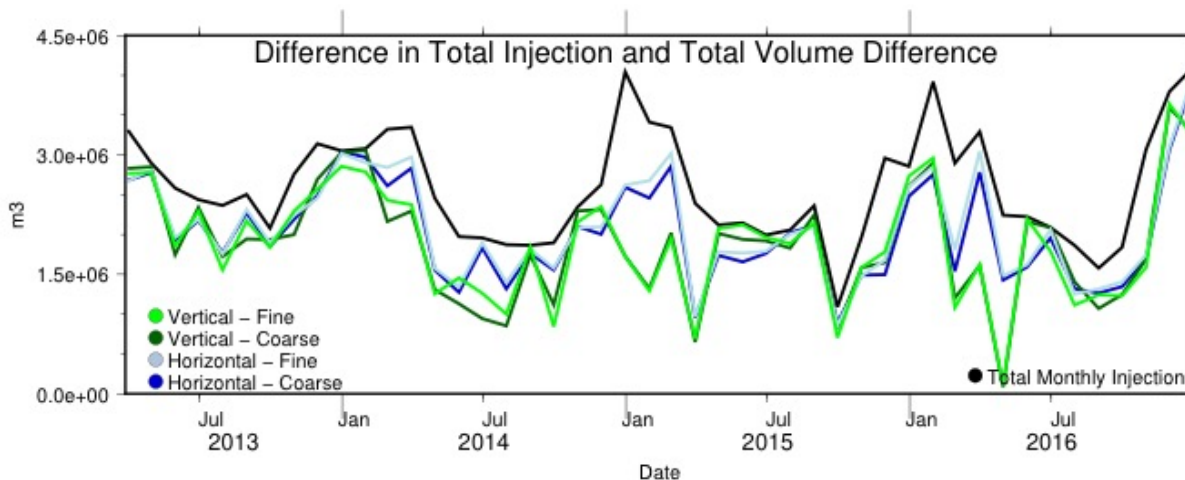


Figure 11: Difference between total injected volume each month and the absolute difference in the total inverted volumes from all four models. There is a larger absolute difference following periods of high injection/reduced overall extraction.

#### 4. Conclusions

In our first attempt to interpret GPS time series data from The Geysers, we use downsampled monthly steam extraction and water/wastewater injection volumes from The Geysers field and input them in to a rectangular elastic dislocation model within an isotropic elastic half space (e.g. Okada 1985). Our four forward models used in this study fail to reproduce the multi-annual trends of our GPS time series data. Possible explanations for why they do not include fluid migration within the reservoir, poroelastic deformation and/or changes in the compressibility of the reservoir. Both models with horizontal dislocations produce a significantly higher amount of vertical deformation than is observed. The average RMS misfit for the conjugate vertical dislocation models is 6 times smaller than for the horizontal dislocation models and is the preferred means of modeling the reservoir.

Using the GPS time series data, we next invert for the opening (dislocation-normal displacement) required at each model dislocation, and therefore the volume changes in the reservoir, that best reproduce the time series data. Since our sparse data coverage provides low model spatial resolution, we summed volume changes for the whole model domain each month to compare those estimated from inverse models to reported well data. The total volume change was similar between all four inverse models and for periods of time was variously in and out of phase with the recorded total volume changes in the field. In the latter cases, the peaks in volume changes estimated in our models lag those from the well data by  $\sim 1$  month. The periods of time when the total volume changes are out of phase occur during periods of high injection volumes, in the winter and early spring. This may indicate a time lag between injection into the wells and the resulting surface deformation that is due to the finite permeability of the reservoir rocks.

#### REFERENCES

- Floyd, M, and Funning, G. "Continuation of survey GPS measurements and installation of continuous GPS sites at The Geysers, California, for geothermal deformation monitoring." (2013): 895-898.
- Garcia, J., Walters, M., Beall, Joe., Hartline, C., Pingol, A., Pistone, Sarah P., and Melinda Wright. "Overview of the northwest Geysers EGS demonstration project." *In Proceedings, Thirty-Seventh Workshop on Geothermal Reservoir Engineering Stanford University.* (2012).
- Gettings, P., R. N. Harris, R. G. Allis, and D. S. Chapman. "Gravity signals at the Geysers geothermal system." *Transactions-Geothermal Resources Council* (2002): 425-430.
- Herring, T., King, R., Floyd, M. and McClusky, S. Introduction to GAMIT/GLOBK, Release 10.6, *Massachusetts Institute of Technology*, Cambridge, Mass., 50 pp. (2015).
- Lofgren, B. "Monitoring crustal deformation in the Geysers-Clear Lake geothermal area, California." No. USGS-OFR-78-597. *Geological Survey*, Sacramento, CA (USA), (1978).
- Mossop, A., and Segall, P. "Subsidence at The Geysers geothermal field, N. California from a comparison of GPS and leveling surveys." *Geophysical Research Letters* 24, no. 14 (1997): 1839-1842.
- Okada, Y. "Surface deformation due to shear and tensile faults in a half-space." *Bulletin of the seismological society of America* 75, no. 4 (1985): 1135-1154.

State of California. "Oil, Gas, and Geothermal." *Division of Oil, Gas, & Geothermal Resources*, State of California, Department of Conservation, (2017), [www.conservation.ca.gov/dog/geothermal/manual/Pages/production.aspx](http://www.conservation.ca.gov/dog/geothermal/manual/Pages/production.aspx).

"The Geysers: A Very Special Place." *The Geysers*, Calpine, 2018 [www.geysers.com](http://www.geysers.com)

Tregoning, P., and Watson, C., "Atmospheric effects and spurious signals in GPS analyses.", *J. Geophys. Res. Solid Earth*, 114, (2009), B09403, doi:10.1029/2009JB006344.

Tregoning, P., and Watson, C. "Correction to "Atmospheric effects and spurious signals in GPS analyses." *J. Geophys. Res. Solid Earth*, (2011), 116, B02412, doi:10.1029/2010JB008157.

Wdowinski, S., Bock, Y., Zhang, J., Fang, P., & Genrich, J. "Southern California permanent GPS geodetic array: Spatial filtering of daily positions for estimating coseismic and postseismic displacements induced by the 1992 Landers earthquake." *Journal of Geophysical Research: Solid Earth*, (1997), 102(B8), 18057-18070.